Available online at www.sciencedirect.com
SCIENCE DIRECT
Optical Materials 28 (2006) 864–867
OPTICAL Materials
www.elsevier.com/locate/optmat

Short-range order around Er^{3+} in silica waveguides containing aluminium, titanium and hafnium

N.D. Afify [a], R. Grisenti [a], G. Dalba [a], C. Armellini [b], M. Ferrari [b], S. Larcheri [b], F. Rocca [b,*], A. Kuzmin [c]

[a] *INFM and Department of Physics, 38050 Povo, Trento, Italy*
[b] *IFN-CNR, Institute for Photonics and Nanotechnologies, Section "ITC-CeFSA" of Trento, 38050 Povo, Trento, Italy*
[c] *Institute of Solid State Physics, University of Latvia, LV-1063 Riga, Latvia*

Available online 3 November 2005

Abstract

Er^{3+}-doped silica waveguides, co-doped with aluminium, titanium, and hafnium oxides, were prepared using the sol–gel method and dip-coating processing. Here, we present a characterisation of the local environment around Er^{3+} ions, as determined from the Er L_3-edge extended X-ray absorption fine structure (EXAFS) measurements performed at ESRF (France). The first coordination shell is composed of 5–6 oxygen atoms at distances ~2.32–2.35 Å, slightly varying as a function of the modifier oxide. Er^{3+} nearest neighbors distance does not show a significant compositional dependence. On the contrary, outer shells analysis shows significant differences: Al_2O_3 doping (less than 2% mol) induces an ordering around Er and increases the distance of the second shell, probably due to the substitution of Si by Al atoms; for TiO_2 doping (7–15% mol), it is most probable that the second shell is composed from Si atoms as the case of pure SiO_2; for HfO_2 doping (from 10 to 50 mol%) there is a very clear evidence of Er–Hf coordination already at the lowest Hf content, but still in amorphous environment.

1. Introduction

Among the different technologies which are employed to develop materials suitable for photonics, sol–gel processing exhibits several advantages in terms of rare-earth solubility, composition, design, tailoring of optical properties as well as fabrication of films, waveguides, photonic crystals, and bulk glasses. The binary silica-based systems, such as silica–titania, silica–hafnia, and silica–alumina, are of particular interest allowing the tailoring of the optical and spectroscopic properties [1]. Information on the nearest and next-nearest coordination shells of the rare-earth ions in the glass host is of crucial importance to design and select the system with optimised spectral properties for fabricating active devices such as planar optical amplifiers.

For this purpose, we present here a comparison between the local structure around Er^{3+} ions in silica glass co-doped with different modifier oxides. In previous publications we presented the local structure around Er^{3+} ions in pure SiO_2 and SiO_2–Al_2O_3 networks [2,3]. We showed that co-doping of SiO_2 with few mol% of Al was sufficient to induce significant changes beyond the first coordination shell. Here we report on new EXAFS experiments on SiO_2–TiO_2 and SiO_2–HfO_2 waveguides. In the last system, in particular, spectroscopic studies have shown a strong modification of the crystal field strength around the Er^{3+} ion, leading to an increase of the electric dipole component of the $^4I_{13/2}$–$^4I_{15/2}$ transition probability [4,5].

2. Experimental and data analysis method

Er^{3+}-doped SiO_2–TiO_2 and SiO_2–HfO_2 solutions with different modifier contents (7, 12, and 15 mol% for TiO_2; 10, 20, 30, 40, and 50 mol% for HfO_2) were prepared using

* Corresponding author. Tel.: +39 461 881685; fax: +39 461 881680.
E-mail address: rocca@science.unitn.it (F. Rocca).

0925-3467/$ - see front matter © 2005 Elsevier B.V. All rights reserved.
doi:10.1016/j.optmat.2005.09.048

Table 1
Structural parameters relative to the first and second coordination shells around erbium in Er^{3+}-doped SiO_2 co-doped with different modifier oxides: N_i, R_i, and σ_i^2 are the coordination number, interatomic distance, and Debye–Waller factor respectively; i stands for shell number (numbers in parenthesis represent the estimated uncertainty on last digit taking into account different best fit parameters)

Sample label	Modifier content (%)	Er^{3+} content (%)	Thermal treatment	N_1 (atom)	R_1 (Å)	σ_1^2 (Å^2)	N_2(atom)	R_2 (Å)	σ_2^2 (Å^2)
	SiO_2			Er^{3+}–O			Er^{3+}–Si		
A	0.0	0.2	900 °C/120 h	4.6(1)	2.32(1)	0.011(1)	4(2)	3.74(1)	0.03(2)
	Al_2O_3			Er^{3+}–O			Er^{3+}–Si(Al)		
B	1.2	0.2	900 °C/120 h	4.8(1)	2.33(1)	0.014(1)	3(1)	3.76(1)	0.02(2)
C	1.8	0.2	900 °C/120 h	5.4(1)	2.35(1)	0.017(1)	3(1)	3.82(1)	0.014(1)
	TiO_2			Er^{3+}–O			Er^{3+}–Si		
D	7	1	900 °C/1 h	5.0(3)	2.33(1)	0.009(1)	3(1)	3.79(2)	0.02(2)
E	12	1	900 °C/1 h	5.1(4)	2.34(1)	0.009(2)	3.5(9)	3.77(1)	0.02(1)
F	15	1	900 °C/1 h	5.1(3)	2.34(1)	0.008(1)	4(1)	3.79(1)	0.02(1)
	HfO_2			Er^{3+}–O			Er^{3+}–Hf		
G	10	0.3	900 °C/30 h	5.1(1)	2.34(1)	0.011(2)	4.0(7)	3.51(1)	0.015(4)
H	20	0.3	900 °C/3.5 h	5.1(1)	2.33(1)	0.012(2)	3.9(7)	3.52(1)	0.013(4)
I	30	0.5	900 °C/5 min	4.8(1)	2.34(2)	0.012(2)	3.4(1)	3.51(1)	0.011(2)
J	40	0.3	900 °C/5 min	5.0(2)	2.33(2)	0.013(2)	3.8(2)	3.50(1)	0.014(4)
K	50	0.3	900 °C/2 min	4.9(2)	2.33(1)	0.012(2)	4.9(9)	3.53(2)	0.020(9)

the sol–gel method and deposited on v-SiO_2 substrates using the dip-coating processing [4]. Composition and thermal history of different samples are compiled in Table 1. X-ray absorption measurements were performed at room temperature (RT) in fluorescence mode at the Er L_3-edge using synchrotron radiation at the BM08 GILDA CRG beamline of ESRF (Grenoble, France) [2,3]. 0.1 M aqueous solution of $Er(NO_3)_3 \cdot 5H_2O$ salt, crystalline $ErVO_4$ and Er_2O_3 powders were also measured in transmission mode as reference compounds. EXAFS data were analysed using the EDA code [6] as described in [6,7]. To model the different EXAFS spectra, we followed the usual Gaussian multi-shell fitting procedure, using either theoretical or experimental backscattering amplitudes and phase shifts. The theoretical ones were calculated using the FEFF8 code [8] and optimized to reproduce the experimental EXAFS signals of the measured reference compounds.

Experimental (dotted lines) Fourier transforms of EXAFS signals $k\chi(k)$ are reported in Fig. 1, together with results of best fits (solid lines). In this figure only one sample is reported for each system due to space limitation; however, the fits of the other samples are of equal quality.

The first coordination shell around Er^{3+}, for all the samples under study, is composed of oxygen atoms; this shell was evaluated using experimental and theoretical backscattering amplitudes and phase shifts extracted from different sources. As experimental scattering functions, we used those extracted from EXAFS spectra at the Er L_3-edge for Er nitrate hydrates water solution, while the theoretical ones were calculated starting from the structure of polycrystalline Er_2O_3. It is worth mentioning here that in previous publications on similar systems, the first shell distances evaluated by us were significantly larger than those reported by D'Acapito et al. [9,10]. In order to verify if such differences were due to our analysis procedures, we have checked the reliability of our results by varying the fitting strategies, scattering functions and so on. In all cases we got values that agree with each other within 0.01 Å as an overall error bar, and our previous results were confirmed [2,3]. The obtained structural parameters relative to the first coordination shell are compiled in Table 1.

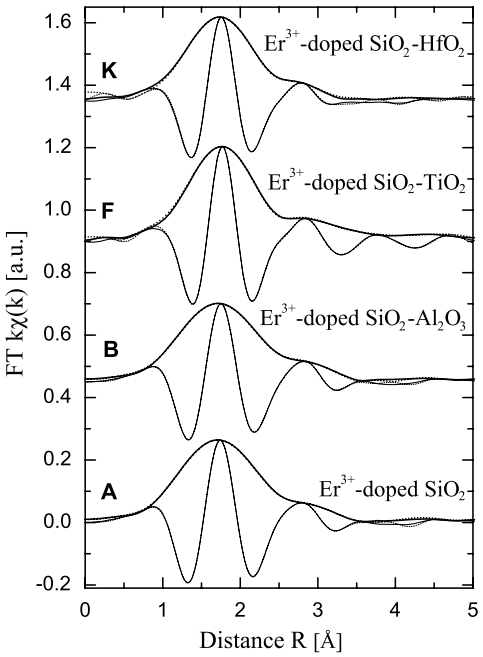

Fig. 1. Experimental (dotted lines) and calculated (solid lines) Fourier transforms of the Er L_3-edge EXAFS signals $k\chi(k)$ with different modifier oxides. Spectra from different systems were vertically shifted for clarity. See text for details.

For the second coordination shell, the backscattering amplitudes and phase shifts for Er–Si, Er–Al, Er–Ti, and Er–Hf atomic pairs were calculated starting from the structure of crystalline $ErVO_4$ by replacing V by Si, Al, Ti and Hf respectively. For each sample, all the possible next-

nearest shell correlations were tested and the plausible solutions were then evaluated. The possibility of the presence of Er → Er coordination was also tried. For all samples, the fit ruled out such correlation at the very beginning, confirming the results of previous EXAFS studies [2,3,9,10].

The structural parameters for the second coordination shell are reported in Table 1, while some examples of the fit are shown in Fig. 1.

As it might be seen from Fig. 1, the quality of best fit is very high, but we should note that the quantitative determination of the outer shells content was in some cases ambiguous. A first reason is due to the fact that the contributions of these shells to the experimental spectra are smeared out by the structural disorder and hence only a short k range of the spectra can be reliably fitted. Another reason is the impossibility to distinguish between the backscattering functions of Al, Si and the high similarity in case of Ti atoms. The most favorable case is that of SiO_2–HfO_2 system, because the backscattering amplitude of hafnium is double-peaked and clearly identifiable.

3. Results and discussion

Let us first discuss the results relative to the first coordination shell of Er^{3+} in the different oxide matrices. From the experimental and calculated Fourier transforms reported in Fig. 1, and the structural parameters compiled in Table 1, the first coordination shell in all the investigated samples is composed of 5–6 oxygen atoms at distances ~2.32–2.35 Å. The first coordination shell is not influenced significantly neither by varying the network modifier nor its concentration. This can be seen as a general trend of Er^{3+}-doped silica glass co-doped with different network modifiers, in case of thermal treatments performed at the same temperature.

The situation in the case of outer coordination shells is much more different and complicated from the first one. The content of the outer shell depends, to a large extent, on type and content of the modifier oxide. The case of pure SiO_2 is the simplest one. Er^{3+} in this case is coordinated only by silicon atoms and the EXAFS signal was best fitted on the basis of a single Er–Si shell centered at ~3.74 Å. The effect of co-doping SiO_2 with Al_2O_3 is documented in Fig. 1: even though the low molar content, the presence of Al atoms leads to considerable changes beyond the first shell. The quantitative analysis (see Table 1), shows an increase in the interatomic distance accompanied by a decrease in the Debye–Waller factor as the aluminium content increases. We observe that the next-nearest shell could be fitted equally well either by silicon or aluminium atoms (due to the strong similarity between backscattering functions). However, the effect of Al co-doping is evident and we confirm our previous interpretation of EXAFS data [2,3]: the ordering and the elongation of the second-shell distance are probably due to the substitution of Si by Al atoms, that are not equally dispersed, but concentrated around the Er^{3+} ions. The resulting "shielding effect" may explain the improvement of optical properties shown by Al co-doped silica gels [12,13].

The identification of the outer shell in the case of SiO_2–TiO_2 was much more complicated, because a single Er^{3+}–Si or Er^{3+}–Ti distance was not able to reproduce the frequencies of the next-nearest shells. Moreover, a distinction between silicon and titanium atoms was impossible on the basis of a multi-shell best fit. We have thus followed an alternative procedure: as a first step, the contribution of the Er^{3+}–O first coordination shell has been evaluated and then subtracted from the whole EXAFS spectrum. The residual was then filtered from noise and reasonable data ranges were estimated for best fitting the outer shells. In this case, only two silicon distances could reproduce, almost perfectly, the residual signal beyond the first shell as shown in Fig. 2. This implies that Er^{3+} is coordinated by silicon atoms as second nearest neighbors. This assumption is supported by the well known fact that in SiO_2–TiO_2, TiO_2 has a known tendency to be phase separated or assume a random-like nature [11]. No detectable effect on the second shell was present by varying TiO_2 content as reported in Table 1.

For co-doping with HfO_2, we have investigated a wide range of composition, on samples where XRD did not show any evidence of nucleation or crystallization. The next-nearest shells are strongly modified by the presence of Hf. The quantitative analysis shows a clear evidence of the presence of hafnium in the second shell, that can be very well fitted by a single distance. The comparison with

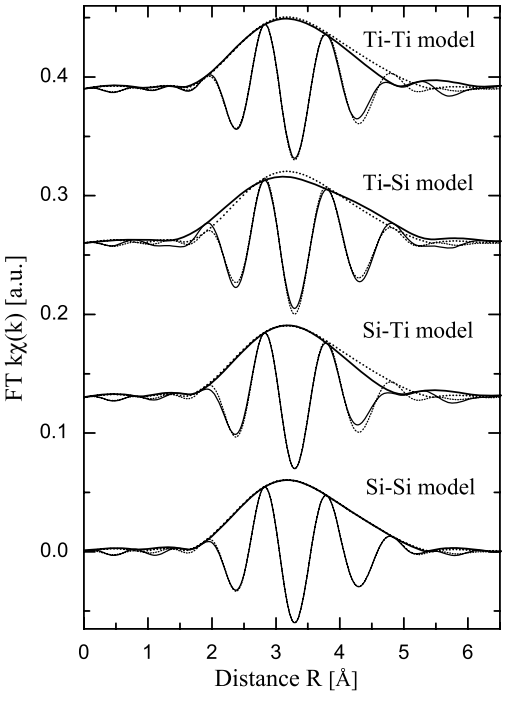

Fig. 2. Fitting of the residual signals corresponding to next-neighbor shells to four models of two distances (experimental (dotted lines) and calculated (solid lines)) as reported for 1% Er^{3+}-doped SiO_2:TiO_2 with 15% TiO_2 as an example.

Al or Ti co-doped samples in Table 1 shows that the Er–Hf distance in the second shell is the shortest one, indicating a densification around Er. EXAFS results indicate that the co-doping with HfO_2 induces a strong modification of the local environment of Er. However, within the explored compositional range, the obtained structural parameters for the second coordination shell remain constant, indicating the presence of HfO_2-rich amorphous regions already at 10 mol% content. The present EXAFS results confirm the conclusions of Ref. [5], where the disruption-role of hafnia on the silica network was supposed to be effective even at low HfO_2 content. Photoluminescence spectra and lifetimes can be explained by considering that the incorporation of HfO_2 in silica strongly modifies the next-nearest shell environment around Er^{3+}, inducing an increase of the electric dipole component of the $^4I_{13/2}$–$^4I_{15/2}$ transition probability.

4. Conclusions

The first coordination shell around erbium in Er^{3+}-doped SiO_2 co-doped with different modifier oxides is composed from 5 to 6 oxygen atoms at distance ~2.32–2.35 Å. This shell is not influenced, significantly, neither by varying the type nor the content of the network modifier.

The situation for the outer coordination shell is very different. The presence of titanium is not detectable in the local environment of erbium. The main effect of co-doping with a low molar content of aluminium is to hamper the clustering of erbium ions, due to the concentration of Al around Er. In the case of SiO_2 co-doped with HfO_2, Er^{3+} ions are mainly dispersed in an amorphous HfO_2 environment, thus explaining why the optical properties are strongly modified with respect to the pure silica wave-guides.

Acknowledgement

This work was partially supported by MIUR, Italy, through the FIRB project ''Sistemi Miniaturizzati per Elettronica e Fotonica''. We are grateful to Luca Zampedri for significant technological and scientific assistance in waveguide fabrication. The financial support by ESRF (F) and INFM (I) is acknowledged. Authors are grateful to the staff of the BM08-GILDA beamline for assistance during the measurements.

References

[1] Handbook of Sol–Gel Science and Technology Processing, Characterization and Applications, H. Kozuka (Ed.), Sol–Gel Processing, vol. I; R.M. Almeida (Ed.), Characterization of Sol–Gel Materials and Products, vol. II; S. Sakka (Ed.), Applications of Sol–Gel Technology, vol. III, 2005, LX, 1980 p. 1100, Hardcover. ISBN: 1-4020-7969-9.
[2] F. Rocca, C. Armellini, M. Ferrari, G. Dalba, N. Diab, A. Kuzmin, F. Monti, J. Sol–Gel Sci. Tech. 26 (2003) 267.
[3] F. Rocca, M. Ferrari, A. Kuzmin, N. Daldosso, C. Duverger, F. Monti, J. Non-Cryst. Solids 293 (2001) 112.
[4] R. Goncalves, G. Carturan, L. Zampedri, M. Ferrari, M. Montagna, A. Chiasera, G. Righini, S. Pelli, S.J.L. Ribeiro, Y. Messaddeq, Appl. Phys. Lett. 81 (2002) 28.
[5] R. Goncalves, G. Carturan, M. Montagna, M. Ferrari, L. Zampedri, S. Pelli, G. Righini, S.J.L. Ribeiro, Y. Messaddeq, Opt. Mater. 25 (2004) 131.
[6] A. Kuzmin, Physica B 208–209 (1995) 175;
A. Kuzmin, J. Phys. IV 7 (1997) C2-213.
[7] A. Kuzmin, J. Purans, J. Phys.: Condens. Matter 12 (2000) 1959.
[8] J.J. Rehr, J. Mustre de Leon, S.I. Zabinsky, R.C. Albers, J. Am. Chem. Soc. 113 (1991) 5135;
J. Mustre de Leon, J.J. Rehr, S.I. Zabinsky, R.C. Albers, Phys. Rev. B 44 (1991) 4146.
[9] F. d'Acapito, S. Mobilio, P. Gastaldo, D. Barbier, L. Santos, O. Marti, R.M. Almeida, J. Non-Cryst. Solids 293 (2001) 118.
[10] F. d'Acapito, S. Mobilio, L. Santos, R.M. Almeida, Appl. Phys. Lett. 78 (2001) 2676.
[11] R.M. Almeida, J. Sol–Gel Sci. Technol. 13 (1998) 51.
[12] A. Chiasera, M. Montagna, R. Rolli, S. Ronchin, S. Pelli, G.C. Righini, R.R. Goncalves, Y. Messaddeq, S.J.L. Ribeiro, C. Armellini, M. Ferrari, L. Zampedri, J. Sol–Gel Sci. Technol. 26 (2003) 943.
[13] A. Monteil, S. Chaussedent, G. Alombert-Goget, N. Gaumer, J. Obriot, S.J.L. Ribeiro, Y. Messaddeq, A. Chiasera, M. Ferrari, J. Non-Cryst. Solids 348 (2004) 44.